ACS OMEGA

http://pubs.acs.org/journal/acsodf

Article

Quantitative Proteomics Analysis of Systemic Responses and Biological Mechanisms of ShuFengJieDu Capsule Using H1N1-Infected RAW264.7 Cells

Zhengang Tao,[#] Jun Chen,[#] Jie Su,[#] Shifei Wu, Ying Yuang, Hebing Yao, Catherine C.L. Wong,* and Hongzhou Lu*

Cite This: *ACS Omega* 2020, 5, 15417−15423

Read Online

ACCESS | Metrics & More | Article Recommendations | Supporting Information

ABSTRACT: Emerging infectious diseases (EIDs) are a significant burden on global economies and public health to any country in the world. With the extensive application of traditional Chinese medicines (TCMs) for EID treatment, the underlying molecular mechanisms have caught more attention than before. The ShuFengJieDu capsule (abbreviated as SFJD) is a TCM prescription used for treating upper respiratory infection (URI) with symptoms of fever, sore throat, headaches, nasal congestion, and cough for more than 30 years in China. SFJD is also widely used for the prevention and treatment of viral infectious diseases, especially for the EIDs. In this study, a bioactivity-integrated method of ultraperformance liquid chromatography quadrapole/time-of-flight mass spectrometry combined with methyl thiazolyl tetrazolium assay was applied to screen potential antivirus compounds in SFJD on the H1N1-infected RAW264.7 cell models. Three compounds (forsythoside E, verbenalin, and emodin) exert the advantages of protective effects in cell vitality during H1N1 infection. The isobaric tags for relative and absolute quantification (iTRAQ)-coupled liquid chromatography coupled to tandem mass spectrometry (LC−MS/MS) analysis and the subsequent quantitative proteome analysis were performed to investigate the potential molecular mechanisms triggered by these three bioactive compound-triggered molecular mechanisms in H1N1-infected RAW264.7 cells. Dysregulated proteins were involved in regulating the levels of proinflammatory cytokines, the IFN (interferon)-stimulated gene signal in the Type I IFN, TBK/IRF3, and MAPK/NF-κB signaling pathways. In conclusion, we identified the main bioactive compounds in SFJD exerting antiviral effects and illuminated that Type I IFN and MAPK/NF-κB signaling pathways are involved in the anti-H1N1 infection effects of SFJD. Our study not only provides solid theoretical support for the clinic application of SFJD but also sheds light on the novel research methods for TCM study.

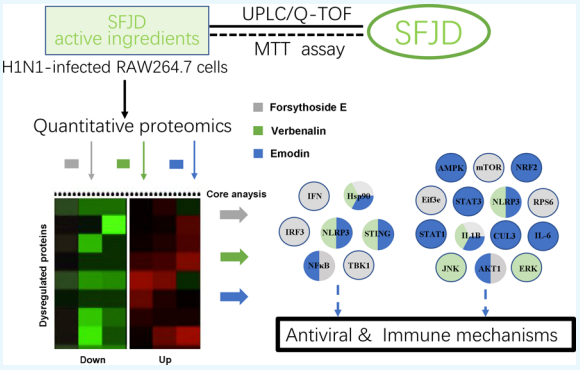

INTRODUCTION

Epidemics associated with emerging infectious diseases (EIDs) are now occurring in historically unprecedented numbers and emerging as a significant burden on global economies and public health.[1] The current main class of antiviral drugs, such as oseltamivir,[2] zanamivir,[3] and peramivir,[4] was approved for treating and preventing influenza worldwide.[5] They comprise a certain chemical constituent and take advantage of clear target and certain biological effects. Although antiviral therapy is an important strategy for controlling influenza, the efficacy depends on the timing of administration and is often limited by supply shortage.[6] Additionally, mutations of the virus have also been found in previous studies to alter the binding property of neuraminidase (NA) for the binding of oseltamivir, making viral strains become resistant against these drugs.[7−9] Thus, more work is still needed to develop new drugs which are simple, effective, and accessible.

In China, the combination of antiviral treatment, such as Tamiflu and traditional Chinese medicines (TCMs), accounted for a large portion and was regarded to have unique advantage in treating EIDs to improve the clinical therapeutic effectiveness in virus prevention and control.[10] The ShuFengJieDu capsule (SFJD), consisting of *Rhizoma polygoni cuspidati*, *Fructus forsythiae*, *Radix isatidis*, *Radix bupleuri*, *Herba patriniae*, *Herba verbenae*, *Rhizoma phragmitis*, and *Radix glycyrrhizae*, is one type of TCM for treating upper respiratory infection (URI) with symptoms of fever, sore throat, headache, and

Received: April 5, 2020
Accepted: June 2, 2020
Published: June 18, 2020

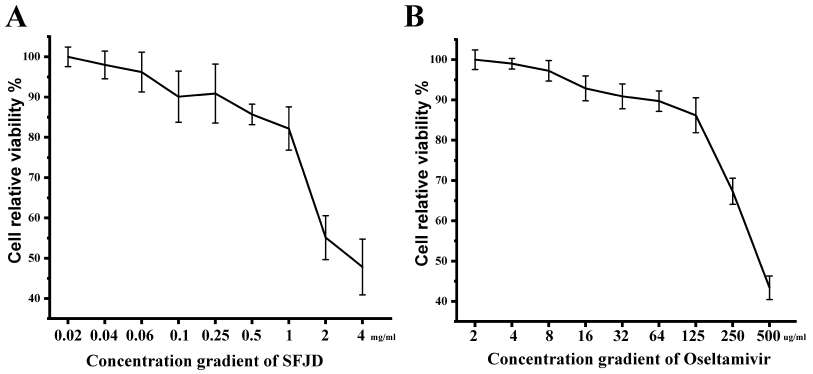

Figure 1. Determination the effects of SFJD on cell viability in RAW264.7 cells. (A) SFJD; (B) oseltamivir. RAW264.7 cells were infected with H1N1 at an MOI of 20 in the treatment of different doses of SFJD or oseltamivir for 24 h. Cytotoxicity of SFJD or oseltamivir to RAW264.7 cells was measured by MTT assays. Data are presented as mean ± SD. The experiments were performed in triplicate.

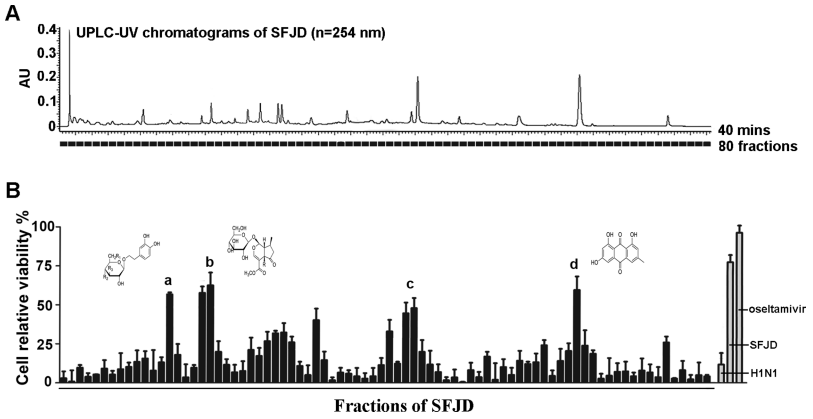

Figure 2. Screening and identification of active ingredients of SFJD in the H1N1-infected RAW264.7 cell line. (A) UPLC-UV chromatograms of SFJD (n = 254 nm). (B) Bioactivity chromatogram obtained via the MTT assay system for cell viability inhibition. Information of the peak numbers (a–d) is shown in Figure S1 and Table S1.

cough.[11−13] A clinical study had demonstrated that administration of SFJD abates fever in an average time of 20.5 h, implying that SFJD had rapid and effective antipyretic action.[14] In our previous study, we found that the presence of SFJD increased the partial pressure of oxygen in lung tissue, decreased lactic acid levels, and inhibited inflammatory factors such as IL-1β and TNF-α in acute lung injury rats. However, the underlying mechanisms remain largely unknown. Moreover, the China Food and Drug Administration (CFDA) has recommended SFJD for the treatment of patients with H1N1- and H5N9-induced flu based on its antiviral effect, but the detailed analysis involved in the component identification of SFJD is still lacking. Thus, it is essential to characterize the medicinal ingredients in SFJD, especially the active ingredients responsible for antiviral effects.

In this study, we investigated the main bioactive compounds exerting antiviral effects in SFJD and uncovered the underlying mechanisms involved in the anti-H1N1 infection effects of SFJD. We assessed the underlying mechanisms of SFJD on regulating the levels of proinflammatory cytokines, the IFN-stimulated gene expressions,[15] and key effectors in the Type I IFN signaling pathways,[16] TBK/IRF3 signaling pathways,[17] and MAPK/NF-κB signaling pathways.[18] Interestingly, forsythoside E, verbenalin, and emodin made distinguishing roles and functions in several certain signals related to antivirus activities, and western blot was finally used to verify related signals. Our studies provide experimental evidence for studying the antivirus mechanism of SFJD and also offer a new way for researchers to find potential natural drugs in TCMs.

RESULTS AND DISCUSSION

Screening and Identification of Active Ingredients in SFJD. The elemental compositions of the active ingredients in SFJD were identified based on the exact molecular weight, compared with data reported in the literature and natural product information references. Each compound was confirmed according to the retention time, MS, and MS/MS fragmentation data from previous studies. The UV chromatograms (254 nm), basic peak ion (BPI) chromatograms in positive/negative ESI modes, and 94 chemical components in SFJD had been shown in our previous study.[11] To determine the proper concentration of SFJD for the further research, we measured its maximum nontoxic concentration. As shown in Figure 1A, the maximum nontoxic concentration of SFJD was 500 μg/mL and the CC_{50} of SFJD was 3064.2 ± 72.01 μg/mL. Oseltamivir was served as a positive control. Its nontoxic concentration was 125 μg/mL and CC_{50} was 397.2 ± 9.42 μg/mL (Figure 1B). SFJD fractions between UPLC and MS had been subdivided into 80 fractions which were collected into 96-well plates every 0.5 min, followed by evaporating to dryness. Then, 200 μL of the cell culture medium was added to dissolve these residues.

To characterize the potential effective components of each fraction from SFJD, the methyl thiazolyl tetrazolium (MTT)

https://dx.doi.org/10.1021/acsomega.0c01545
ACS Omega 2020, 5, 15417−15423

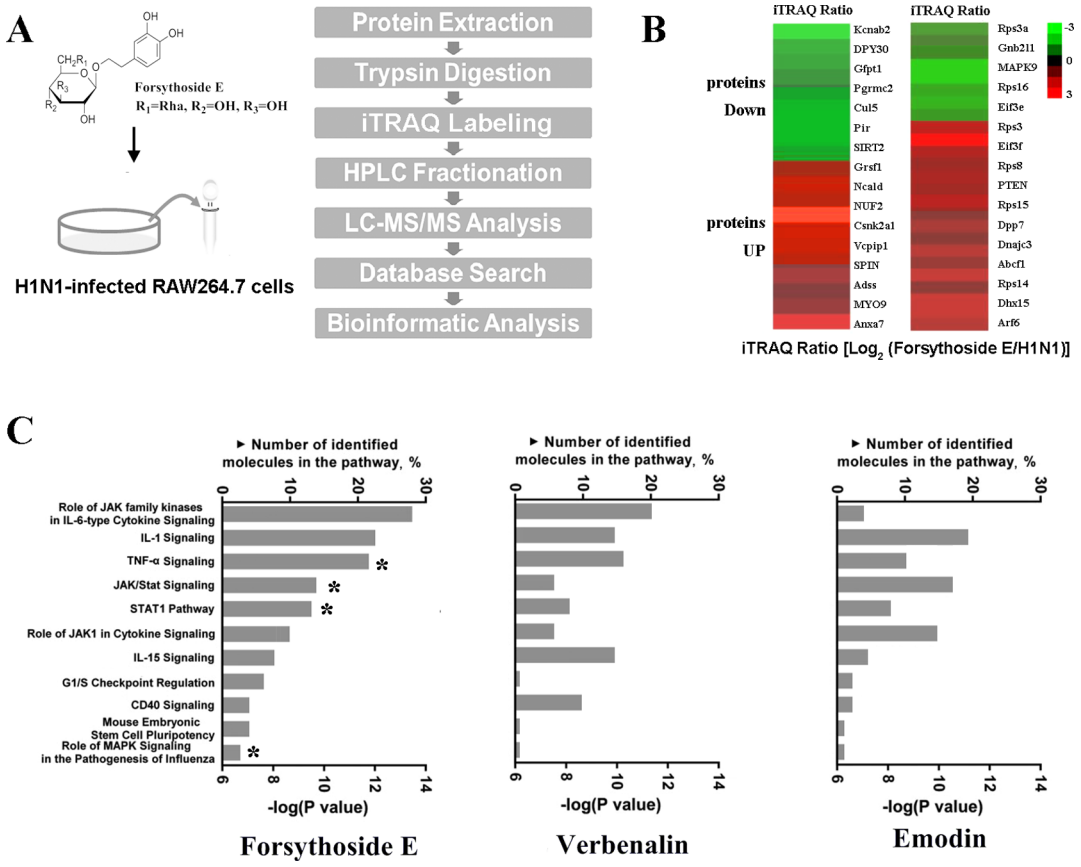

Figure 3. Quantitative proteomics approach to reveal novel mechanisms of those active ingredients in the H1N1 infection in RAW264.7 cells. (A) Workflow of the iTRAQ approach for the three candidate ingredients, respectively (*e.g.*, forsythoside E). (B) Expression levels of 105 proteins (partial) in the forsythoside E-treated group showed significant differences (log_2[forsythoside E/H1N1], ≤0.66 or ≥1.5 and $p < 0.05$). (C) Cell signal core analysis related with antivirus and immunoregulation of the three candidate ingredients.

method was used to investigate the cell activity (the oseltamivir group was set up as the positive control). As shown in Figure 2, the SFJD group (1 mg/mL) resulted in an increase in cell viability (76.34 ± 3.64%) compared to the H1N1 group. The cell relative viability of the oseltamivir group (0.8 mg/mL) was 93.34 ± 2.84% (normal control, RAW264.7 cell line, regarded as 100% cell relative viability). Among the fraction-treatment groups, cell viabilities in several groups, including forsythoside E (fractions no. 14, 57.03 ± 2.12%), verbenalin (fractions no. 19, 61.23 ± 4.42%), and emodin (fractions no. 64, 58.34 ± 7.14%), were significantly enhanced by about 50% (Table S1).

Protein Profiles Reveal Global Protein Changes in Different Treatment Groups in the H1N1-Infected RAW264.7 Cells. To gain the insight into systemic responses to H1N1 virus infection in the absence or presence of forsythoside E, verbenalin, or emodin, we used a quantitative proteomics approach to reveal novel mechanisms of these active ingredients, respectively. The isobaric tag for relative and absolute quantitation (iTRAQ) approach was employed to analyze the protein changes in the three candidate ingredient (forsythoside E, verbenalin, and emodin)-treated groups. As shown in Figure 3A, the workflow of the iTRAQ approach was used for the three candidate ingredients, respectively (forsythoside E, verbenalin, and emodin). Compared with those in the nontreated H1N1-infected RAW264.7 group, the expression levels of 105 proteins in the forsythoside E-treated group showed significant differences (63 upregulated and 42 downregulated) (Table S2) (Figure 3B). To get a more precise analysis, we focused on the cell signals related with antivirus and immunoregulation in IPA core analysis. Taking the forsythoside E-treated group as an example, an overview of biological processes and signaling pathways in the forsythoside E-treated group is shown in Figure 3C. Furthermore, based on our dataset, a total of 33 differentially expressed proteins fell into this "antivirus and immune-regulation" category (Table S2). These proteins were involved in IL-1/TNF-α signaling, JAK/STAT signaling, and MAPK signaling. In the antivirus- and immune-regulation-related pathway, three key proteins, NF-$\kappa\beta$, MAPK, and STAT1, were selected for the validations by the western blot method. The phosphorylated $MAPK_{P38}$, STAT1, and $NF\text{-}\kappa B_{p65}$ are the key signaling molecules in the Type I interferons (IFNs).[19−21] To our knowledge, Type I IFNs are essential for immune defense against viruses.[22] Macrophages infected by influenza virus can synthesize and release proinflammatory cytokines and IFNs, which further limit viral replication and spread.[23] Intriguingly, single ingredient showed various effects in H1N1-infected RAW264.7 cells (Figure 3C).

Type I IFN-Related Signaling Pathway Analysis in SFJD-Treated H1N1-Infected RAW264.7 Cells. The dysregulated core regulators in forsythoside E-, verbenalin-, or emodin-treated groups were integrated according to the related signals in antivirus and immune mechanism. Through analyzing the abovementioned data, we found that Type I IFN-related signals occupied a lot of proportion in a variety of signal categories. Type I IFNs are the major line of host defense

https://dx.doi.org/10.1021/acsomega.0c01545
ACS Omega 2020, 5, 15417−15423

against viruses and other microorganisms. Viral RNA activates signaling cascades through a number of pattern recognition receptor (PRR)−adaptor protein pairs, including RIG-I−MAVS, cGAS-STING, and TLR3/4-TRIF (toll-like receptors 3 and 4).[24,25] Type I IFNs are regulated by IFN regulatory factor 3 (IRF-3), nuclear factor kappa B subunit p65 (NF-κB_{p65}), and several intracellular signaling molecules, which are activated by PRRs.[21] Type I IFNs are essential for immune defense against viruses by inducing the expression of interferon-stimulated genes and then suppressing the replication and spread of virus.[20] Type I IFNs activate key components of the innate and adaptive immune systems, which are well-studied cytokines with antiviral and immune-modulating functions.[21]

The most studied members of the Type I family of interferons are the multiple IFNα and IFNβ. Interferon regulatory factor 3 (IRF3) is a transcription factor of IFN-β. In the early phase of viral infection, IκB kinase ε and TANK-binding kinase 1 (TBK-1) phosphorylate IRF3 lead to the activation and homodimerization of the molecule. The phosphorylation of IRF3 indicates the translocation of IRF3 molecules into the nucleus and the initiation of the transcription of Type I IFNs.[25]

Simultaneously, the synthesized IFN-β initiates JAK-STAT signaling during virus infection, leading to the phosphorylation of STAT1 and giving rise to a major contribution of IFN-induced genes (ISGs).[26] NF-κB, a transcription factor in the immune response, translocates into the nucleus and initiates the induction of genes involved in inflammatory responses.[23]

To further explore the underlying antiviral mechanisms of SFJD, we examined the expressions of the Type I IFN and PRR-related protein phosphorylation. Western blot analysis was performed using the lysates of H1N1-infected RAW264.7 cells treated with or without target ingredients (forsythoside E, verbenalin, or emodin) to determine the protein expressions of the phosphorylated and nonphosphorylated forms of TBK1, IRF3, $MAPK_{P38}$, and NF-κB_{p65}. TBK1 (TANK-binding kinase-1) is a kinase downstream of critical adaptors in the cytoplasmic DNA- and RNA-sensing pathways, which phosphorylates transcription factor interferon regulatory factor 3 (IRF3). As shown in Figure 4, the ratio of *p*-TBK1/TBK1, *p*-IRF3/IRF3, and p-NF-κB_{p65}/NF-κB in the H1N1-infected group was markedly higher in comparison with that in the uninfected group ($p < 0.01$). Compared with the H1N1-infected group, protein expressions of the phosphorylated forms of TBK1, IRF3, $MAPK_{p38}$, and NF-κB_{p65} in the forsythoside E-treated group were significantly downregulated.

Here, key molecules (IRF3, MAPK, and NF-κB) mediating the Type I IFN response and MAPK/NF-κB signaling pathways were upregulated under H1N1 infection, while the increased trend was abrogated when H1N1-infected RAW264.7 cells were treated with SFJD. These results provide the first evidence for the effects of SFJD against H1N1 virus *via* quantitative proteomics methods, suggesting that SFJD could mediate the protein phosphorylation levels of the H1N1-induced Type I IFNs and PRR signaling pathways to enhance its antiviral function *in vitro*.

CONCLUSIONS

In this study, the main bioactive compounds (forsythoside E, verbenalin, and emodin) in SFJD exerting antiviral effects were identified. They remarkably increased the cell viability of H1N1-infected RAW264.7 cells. Further mechanism study reveals that Type I IFNs and MAPK/NF-κB signaling pathways are involved in the anti-H1N1 infection effects of SFJD. Our study not only provides solid theoretical support for the clinical application of SFJD but also sheds light on the novel research methods for TCM study.

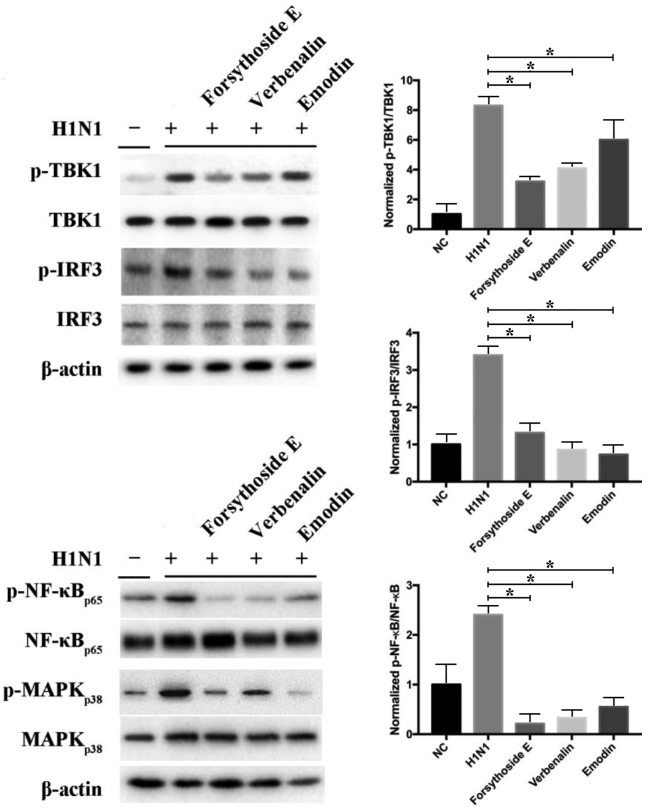

Figure 4. Western blot of Type I IFN-related proteins in the H1N1-infected RAW264.7 cells. For all the experimental groups, RAW264.7 cells were infected with H1N1 at an MOI of 20. The expression level of phosphorylated MAPK, STAT1, and NF-κB and total IRF3, MAPK, and NF-κB was analyzed by western blot d at 24 h. $n = 3$ for each test. * indicates $p < 0.05$.

MATERIALS AND METHODS

Reagents and Materials. SFJD (China State Food and Drug Administration—drug approval number: Z20090047, executive standard number: YBZ00652009) was provided by Anhui Jiren Pharmaceutical CO., LTD (Anhui, China). The preparation and quality control of SFJD has been performed by our previous study (11), and the components of SFJD were detected by high-performance liquid chromatography (HPLC) (Supporting Information). Oseltamivir phosphate capsules (Lot: SH0037) were purchased from Roche Pharmaceutical Co., Ltd. (Shanghai, China). Antibodies against phospho-NF-κB p65 (p-NF-κB p65) and NF-κB p65 were purchased from Abcam (Cambridge, UK). Phospho-IRF3 (*p*-IRF3), IRF3, phosphosignal transducers and activators of transcription 1 (p-STAT1), STAT1, phospho-TANK-binding kinase 1 (*p*-TBK1), TBK1 phosphomitogen-activated protein kinases (*p*-MAPK P38), MAPK P38, phospho-extracellular regulated protein kinases (*p*-ERK), ERK, and β-actin antibodies were purchased from Santa Cruz Biotechnology (CA, USA).

Bioactivity-Based UPLC/Q-TOF for Active Ingredient Identification in SFJD. A Waters Acquity UPLC instrument system (Waters Co., USA) was used to separate the SFJD

https://dx.doi.org/10.1021/acsomega.0c01545
ACS Omega 2020, 5, 15417−15423

sample, which was equipped with a 2.1 mm × 100 mm, 1.7 μm BEH C18 column (Waters, UK). The column temperature was maintained at 30 °C and UV detection was performed over the range of 190−400 nm. The mobile phases A and B were acetonitrile and water with 0.1% formic acid, respectively. The flow rate was 0.4 mL/min, the injection volume was 10 μL and the gradient duration program was as follows: 0−2 min, 2% A; 2−12 min, 2−15% A; 12−15 min, 15% A; 15−18 min, 15−20% A; 18−35 min, 20−50% A; and 35−40 min, 50−100% A. The mass spectrum was acquired with a Waters Q-TOF Premier coupled to an electrospray ionization source (Waters MS Technologies, Manchester, UK) in both the negative and positive ion voltage modes. The MS acquisition range was from 50 to 1500 m/z. The source temperature was set at 100 °C and the desolvation temperature was maintained at 300 °C with the desolvation gas flow rate at 600 L/h. The capillary voltage was 2.5 kV for the negative mode and 3.0 kV for the positive mode, and the sample cone voltage was 30 V, the collision energy was 5 eV, and the cone gas was 50 L/h. Leucine-enkephalinamide acetate (LEA, 200 ng/mL) was used as the lock mass (m/z 555.2931 in ESI^+ and 553.2775 in ESI^-) with the flow rate of 20 μL/min.

Viruses and Cell Culture. Mouse-adapted influenza virus A/PR/8/34 (H1N1) was kindly donated by Professor Li-Yang from Shanghai University of Chinese Medicine. Virus was propagated in the allantoic cavities of 9 day-old specific-pathogen-free (SPF) chicken embryonated eggs. After further incubation for 48 h at 37 °C, allantoic fluids containing the viruses were harvested. The viruses were divided into small portions and stored at −80 °C until use. Virus titers were calculated by the Reed−Muench method and expressed as median tissue infectious doses ($TCID_{50}$). The murine macrophage cell line (RAW264.7) was purchased from the Type Culture Collection of the Chinese Academy of Sciences, Shanghai, China. RAW264.7 cells were cultured in Dulbecco's modified Eagle's medium (DMEM) (Gibco, Grand Island, NY, USA). The media was supplemented with 10% inactivated fetal bovine serum (Gibco) and antibiotics (100 U/mL penicillin G and 100 μg/mL streptomycin) (Gibco). The cells were incubated in a humidified atmosphere containing 5% CO_2 at 37 °C. After RAW264.7 cells were infected with influenza virus (multiplicity of infection, MOI = 20), the virus growth medium (serum-free DMEM medium) was supplemented with 2 μg/mL L-1-(tosyl-amido-2-phenyl) ethyl chloromethyl ketone (TPCK)-treated trypsin (Sigma).

Screening and Identification of Chemical Components in SFJD. SFJD (One-gram weight) was extracted with 20 mL of 70% methanol using an Ultrasonic cleaner (40 kHz, 500 W, Ningbo, China) for 20 min at room temperature. The extract was centrifuged at 13,000 rpm for 10 min at 4 °C and the supernatants were filtered through a membrane filter (0.22 μm) for UPLC-TOF MS analysis. A total of 94 compounds of SFJD were identified and fingerprint chromatography including 22 mutual peaks was established with the similarity of more than 0.9.Related files and 94 chemical components in SFJD were also deposited in an online data repository as an attachment file (http://www.iprox.org), the project id being IPX0000995002.

Cell Viability Assay. Cell viability in all experiments was evaluated using the MTT method. Cells (1×10^5 cells/well) were seeded in 96-well plates (Corning Incorporated, USA). After incubating for 24 h, RAW264.7 cells were infected with influenza virus for 1 h and then the medium was removed, and RAW264.7 cells were added with serially diluted SFJD fractions, and all drugs were diluted in serum-free medium. After 24 h treatment, 20 μL/well MTT solution (5 mg/mL in PBS) was added, and the cells were further incubated for an additional 4 h. Formazan precipitates were dissolved with dimethyl sulfoxide (150 μL/well), and then, the absorbance was measured at 490 nm with a microplate reader (Bio-Rad model 680, O-524). The cell viability of normal groups (RAW264.7, NC group) was set at 100%, and the treated samples were normalized to this value (H1N1-infected RAW264.7 cells, H1N1 group). Cell viability according to the following equation: cell survival (%) = optical density (OD) of treated cells/OD of normal control × 100. The 50% cytotoxic concentration (CC_{50}) was calculated as the concentration of SFJD causing the death of 50% of the cells.

Isobaric Tag for Relative and Absolute Quantitation. At 24 h after treatment, cells were collected and lysed, and the protein concentration was determined by BCA assay (Pierce, Rockford, IL) for the further iTRAQ analysis. iTRAQ reagents were purchased from Applied Biosystems (Foster City, CA). Tris (2-carboxyethyl) phosphine hydrochloride (TCEP), trifluoro-acetic acid (TFA), HPLC-grade acetonitrile (ACN), and 4-(2-hydroxyethyl)-1-piperazineethanesulfonic acid (HEPES) were from Sigma-Aldrich (St. Louis, MO) (more information in the Supporting Information).

Functional Enrichment Analysis. The significantly up- and downregulated proteins in the different treatment groups were used to analyze enriched functions using ingenuity pathway analysis (IPA) software (Ingenuity Systems, Redwood City, CA) and gene ontology (GO) databases (more information in the Supporting Information).

Western Blot Assay. Cells were washed twice with chilled PBS and then lysed in RIPA lysis buffer (Beijing Bey time Biotech Co., Ltd., Lot: 00021304) containing a protease inhibitor. Monomeric acrylamide/bisacrylamide solution (40%, 29:1), ammonium persulfate, and protein assay dye were from Bio-Rad (Hercules, CA). Trypsin (modified, sequencing grade) was from Promega (Madison, WI). Water was obtained from a Milli-Q Ultrapure water purification system (Millipore, Billerica, MA). All experiments were repeated three times. The lysis solution was on ice for 30 min. Obtained cell lysates were centrifuged at 12,000g for 15 min at 4 °C to remove debris, and protein concentration in the supernatants was measured using the BCA protein assay kit (Beijing Bey time Biotech Co., Ltd., Lot: 00041305). Each sample was separated by denaturing sodium dodecyl sulfate polyacrylamide gel electrophoresis (SDS-PAGE) and transferred to a PVDF membrane by electrophoretic transfer. The membrane was blocked with 5% nonfat milk and 0.05% Tween-20 in Trisbuffered saline (TBST) and then incubated with the primary antibody at 4 °C overnight. After washing three times for 10 min, the PVDF membrane was incubated with horseradish peroxidase-conjugated anti-rabbit IgG at room temperature for 2 h. The blots were visualized with the ECL reagent (GE Healthcare, Pisca-taway, NJ). The gel images were performed with the ChemiDoc XRS^+ analysis software.

Statistical Analysis. Statistical analysis for multiple group comparisons was performed by one-way analysis of variance (ANOVA) and expressed as the mean ± standard deviation (SD). The p values less than 0.05 were considered as statistically significant ($^*p < 0.05$).

Additional material and methods are shown in the Supporting Information.

https://dx.doi.org/10.1021/acsomega.0c01545
ACS Omega 2020, 5, 15417−15423

■ ASSOCIATED CONTENT

Supporting Information

The Supporting Information is available free of charge at https://pubs.acs.org/doi/10.1021/acsomega.0c01545.

Chemical structural formula of forsythoside E, verbenalin, and emodin; MSMS data in (±) ESI modes and the identification results for the bioactive compounds of SFJD; global protein changes in different treatment groups during the H1N1 infection in RAW264.7 cells (PDF)

(XLSX)

■ AUTHOR INFORMATION

Corresponding Authors

Catherine C.L. Wong − *Center for Precision Medicine Multiomics Research, Peking University Health Science Center, Beijing 100191, China;* orcid.org/0000-0001-7270-980X; Email: catherine_wong@bjmu.edu.cn; Fax: +86-2077-8073

Hongzhou Lu − *Shanghai Public Health Clinical Center, Fudan University, Shanghai 200433, China; Department of Infectious Disease, Huashan Hospital Affiliated to Fudan University, Shanghai, China;* orcid.org/0000-0003-1846-5431; Email: luhongzhou@fudan.edu.cn; Fax: +86-2077-8881

Authors

Zhengang Tao − *Department of Emergency, Affiliated Zhongshan Hospital, Fudan University, Shanghai 200032, China*

Jun Chen − *Department of Infectious Diseases and Shanghai Public Health Clinical Center, Fudan University, Shanghai 200433, China*

Jie Su − *Shanghai Institute for Advanced Immunochemical Studies, ShanghaiTech University, Shanghai 201210, China*

Shifei Wu − *Center for Precision Medicine Multiomics Research, Peking University Health Science Center, Beijing 100191, China*

Ying Yuang − *Department of Presbyatrics, Affiliated Zhongshan Hospital, Fudan University, Shanghai 200032, China*

Hebing Yao − *Shanghai Institute for Advanced Immunochemical Studies, ShanghaiTech University, Shanghai 201210, China*

Complete contact information is available at: https://pubs.acs.org/10.1021/acsomega.0c01545

Author Contributions

#Z.T., J.C., and J.S. contributed equally to this work.

Notes

The authors declare no competing financial interest.

■ ACKNOWLEDGMENTS

This research was supported by the Shanghai Municipal Health Commission (no. ZHYY-ZXYJHZX-1-201703), the National Key Research and Development Project (grant no. 2018YFE0102300), and the National Natural Science Foundation of China (nos. 81773967 and 81803805). Helpful discussions with Prof. Li-Yang, Prof. Tie-Jun Zhang, and Dr. Zhi-Kun are gratefully acknowledged. The data analyses were facilitated by access to the Center for Precision Medicine Multi-omics Research Health Science Center, Peking University (CPMMR).

■ ABBREVIATIONS

LC−MS/MS, liquid chromatography coupled to tandem mass spectrometry; iTRAQ, isobaric tags for relative and absolute quantification; TBK1, TANK-binding kinase 1; IRF3, IFN-regulatory factor 3; SPF, specific-pathogen free

■ REFERENCES

(1) Jones, K. E.; Patel, N. G.; Levy, M. A.; Storeygard, A.; Balk, D.; Gittleman, J. L.; Daszak, P. Global trends in emerging infectious diseases. *Nature* **2008**, *451*, 990−993.

(2) McClellan, K.; Perry, C. M. Oseltamivir. *Drugs* **2001**, *61*, 263−283.

(3) Dunn, C. J.; Goa, K. L. Zanamivir. *Drugs* **1999**, *58*, 761−784.

(4) Smee, D. F.; Sidwell, R. W. Peramivir (BCX-1812, RWJ-270201): potential new therapy for influenza. *Expert Opin. Invest. Drugs* **2002**, *11*, 859−869.

(5) Cooper, N. J.; Sutton, A. J.; Abrams, K. R.; Wailoo, A.; Turner, D.; Nicholson, K. G. Effectiveness of neuraminidase inhibitors in treatment and prevention of influenza A and B: systematic review and meta-analyses of randomised controlled trials. *Br. Med. J.* **2003**, *326*, 1235.

(6) Hui, D. S.; Lee, N.; Chan, P. K. S. Clinical management of pandemic 2009 influenza A(H1N1) infection. *Chest* **2010**, *137*, 916−925.

(7) Moscona, A. Global transmission of oseltamivir-resistant influenza. *N. Engl. J. Med.* **2009**, *360*, 953−956.

(8) Russell, R. J.; Haire, L. F.; Stevens, D. J.; Collins, P. J.; Lin, Y. P.; Blackburn, G. M.; Hay, A. J.; Gamblin, S. J.; Skehel, J. J. The structure of H5N1 avian influenza neuraminidase suggests new opportunities for drug design. *Nature* **2006**, *443*, 45−49.

(9) Collins, P. J.; Haire, L. F.; Lin, Y. P.; Liu, J.; Russell, R. J.; Walker, P. A.; Skehel, J. J.; Martin, S. R.; Hay, A. J.; Gamblin, S. J. Crystal structures of oseltamivir-resistant influenza virus neuraminidase mutants. *Nature* **2008**, *453*, 1258−1261.

(10) Ge, H.; Wang, Y.-F.; Xu, J.; Gu, Q.; Liu, H.-B.; Xiao, P.-G.; Zhou, J.; Liu, Y.; Yang, Z.; Su, H. Anti-influenza agents from Traditional Chinese Medicine. *Nat. Prod. Rep.* **2010**, *27*, 1758−1780.

(11) Tao, Z.; Meng, X.; Han, Y.-q.; Xue, M.-m.; Wu, S.; Wu, P.; Yuan, Y.; Zhu, Q.; Zhang, T.-J.; Wong, C. C. L. Therapeutic Mechanistic Studies of ShuFengJieDu Capsule in an Acute Lung Injury Animal Model Using Quantitative Proteomics Technology. *J. Proteome Res.* **2017**, *16*, 4009−4019.

(12) Li, Y.; Chang, N.; Han, Y.; Zhou, M.; Gao, J.; Hou, Y.; Jiang, M.; Zhang, T.; Bai, G. Anti-inflammatory effects of Shufengjiedu capsule for upper respiratory infection via the ERK pathway. *Biomed. Pharmacother.* **2017**, *94*, 758−766.

(13) Ji, S.; Bai, Q.; Wu, X.; Zhang, D. W.; Wang, S.; Shen, J. L.; Fei, G. H. Unique synergistic antiviral effects of Shufeng Jiedu Capsule and oseltamivir in influenza A viral-induced acute exacerbation of chronic obstructive pulmonary disease. *Biomed. Pharmacother.* **2020**, *121*, 109652.

(14) Sawakami, T.; Xia, J.; Song, P. Researchers of chronic obstructive pulmonary disease gathered at the 2017 Japan-China Joint Medical Workshop on Aging and Health. *BioSci. Trends* **2017**, *11*, 706−709.

(15) Itsui, Y.; Sakamoto, N.; Kurosaki, M.; Kanazawa, N.; Tanabe, Y.; Koyama, T.; Takeda, Y.; Nakagawa, M.; Kakinuma, S.; Sekine, Y.; Maekawa, S.; Enomoto, N.; Watanabe, M. Expressional screening of interferon-stimulated genes for antiviral activity against hepatitis C virus replication. *J. Viral. Hepat.* **2006**, *13*, 690−700.

(16) Mancuso, G.; Midiri, A.; Biondo, C.; Beninati, C.; Zummo, S.; Galbo, R.; Tomasello, F.; Gambuzza, M.; Macrì, G.; Ruggeri, A.; Leanderson, T.; Teti, G. Type I IFN signaling is crucial for host resistance against different species of pathogenic bacteria. *J. Immunol.* **2007**, *178*, 3126−3133.

(17) Korherr, C.; Gille, H.; Schafer, R.; Koenig-Hoffmann, K.; Dixelius, J.; Egland, K. A.; Pastan, I.; Brinkmann, U. Identification of proangiogenic genes and pathways by high-throughput functional

genomics: TBK1 and the IRF3 pathway. *Proc. Natl. Acad. Sci. U.S.A.* **2006**, *103*, 4240−4245.
(18) Meng, Z.; Yan, C.; Deng, Q.; Gao, D.-f.; Niu, X.-l. Curcumin inhibits LPS-induced inflammation in rat vascular smooth muscle cells in vitro via ROS-relative TLR4-MAPK/NF-kappaB pathways. *Acta Pharmacol. Sin.* **2013**, *34*, 901−911.
(19) Perry, A. K.; Chen, G.; Zheng, D.; Tang, H.; Cheng, G. The host type I interferon response to viral and bacterial infections. *Cell Res.* **2005**, *15*, 407−422.
(20) Schoggins, J. W. Interferon-stimulated genes: roles in viral pathogenesis. *Curr. Opin. Virol.* **2014**, *6*, 40−46.
(21) Takeuchi, O.; Akira, S. Pattern recognition receptors and inflammation. *Cell* **2010**, *140*, 805−820.
(22) Lin, R.-J.; Liao, C.-L.; Lin, E.; Lin, Y.-L. Blocking of the alpha interferon-induced Jak-Stat signaling pathway by Japanese encephalitis virus infection. *J. Virol.* **2004**, *78*, 9285−9294.
(23) Palma, J. P.; Kwon, D.; Clipstone, N. A.; Kim, B. S. Infection with Theiler's murine encephalomyelitis virus directly induces proinflammatory cytokines in primary Astrocytes via NF-kappa B activation: Potential role for the initiation of demyelinating disease. *J. Virol.* **2003**, *77*, 6322−6331.
(24) Iwasaki, A.; Pillai, P. S. Innate immunity to influenza virus infection. *Nat. Rev. Immunol.* **2014**, *14*, 315−328.
(25) Kawai, T.; Akira, S. The role of pattern-recognition receptors in innate immunity: update on Toll-like receptors. *Nat. Immunol.* **2010**, *11*, 373−384.
(26) Liu, J.; HuangFu, W.-C.; Kumar, K. G. S.; Qian, J.; Casey, J. P.; Hamanaka, R. B.; Grigoriadou, C.; Aldabe, R.; Diehl, J. A.; Fuchs, S. Y. Virus-induced unfolded protein response attenuates antiviral defenses via phosphorylation-dependent degradation of the type I interferon receptor. *Cell Host Microbe* **2009**, *5*, 72−83.

https://dx.doi.org/10.1021/acsomega.0c01545
ACS Omega 2020, 5, 15417−15423